3D Reconstruction of Grassland Landforms Using Intelligent Robot Vision and Numerical Simulation

Min Zhong[1,2], Zhanxue Zhou[2*]
[1]School of Architecture and Engineering, Jiangsu Open University, Nanjing, Jiangsu, 210036, China
[2]Civil Engineering College, Hebei University of Architecture, Zhangjiakou, Hebei, 075000, China
E-mail: zzx1493@hebiace.edu.cn
[*]Corresponding author

Keywords: characteristic numerical simulation, grassland landform, intelligent robot vision system, three-dimensional reconstruction

Recieved: May 29, 2024

Grassland is an important component in the natural ecosystem. Geological detection and numerical analysis of grassland landforms are the main ways to protect and develop grassland ecological environment. However, the traditional grassland geological survey is not effective. The displayed grassland landforms are not intuitive and the numerical fitting accuracy is low, seriously affecting the work efficiency of grassland landform survey. With the development of machine vision, cloud computing and other technologies, the intelligent robot vision system has stable spatial positioning and construction capabilities. Using the intelligent robot vision system, the grassland landform was reconstructed in 3D (three-dimension) and compared with the traditional grassland landform construction. The experimental results showed that the accuracy of the 3D modeling based on the intelligent robot vision system and the traditional 3D reconstruction in the sixth test of the square grassland with a side of 2km was 96% and 72% respectively. In a square grassland area with a side length of 2km, the average matching degrees of the two 3D modeling feature data were 89.3% and 73.3% respectively. The study conclude that 3D reconstruction of grassland landforms based on the intelligent robot vision system can greatly shorten the time of 3D reconstruction and improve the efficiency of 3D reconstruction of grassland landforms.

Povzetek: Narejena je 3D rekonstrukcijo travniških reliefov z uporabo inteligentnega robotskega vidnega sistema, kar izboljša točnost in učinkovitost geoloških analiz v primerjavi s tradicionalnimi metodami.

1 Introduction

With the continuous development of industrial technology, the quality and scale of the natural ecological environment are declining year by year. Ecological environment detection is a data description of the quality of the ecological environment. Among them, grassland landforms are one of the main ecological environments. The detection of grassland landforms can help protect the grassland environment, maintain the diversity of grassland species, and effectively predict and analyze grassland geological changes. In the traditional grassland landform detection process, the landform analysis or simple three-dimensional analysis is performed in two-dimensional forms such as drawing a plan, a broken line, and a profile. However, the data cannot fully display the complex grassland geological data, wasting a lot of detection time, and the obtained grassland landform detection effect is very poor. With the development of intelligent technology, robot vision and other technologies are combined with multiple fields. Computer vision system technology has super-strong spatial 3D construction capabilities, which can accurately reconstruct grassland landforms in 3D by analyzing the characteristic data of grassland landforms. Applying the intelligent computer vision system to the geological survey of grassland landforms can establish an accurate three-dimensional model, improve the accuracy of grassland feature data analysis, and improve the work efficiency of grassland landform geological survey. Therefore, this paper has research significance.

Geological detection of grassland landforms is conducive to maintaining the grassland ecological environment. Many people have carried out three-dimensional reconstruction and characteristic data simulation of grassland landforms. Among them, Huang Y's research showed that three-dimensional construction of grassland landforms was carried out, and the structural composition of grassland landforms was analyzed, which improved the targeted protection of grassland environment [1]. Sun R conducted three-dimensional modeling and analysis of a variety of grassland types, and the species of grassland was gradually decreasing [2]. Zhang J M carried out three-dimensional modeling of grassland geological soil, and obtained the composition of grassland soil through visual analysis [3]. Xu Y's research pointed out that 3D

reconstruction of grassland landforms can improve the accuracy of geological detection and improve the detection efficiency [4]. According to Sui D's research, the analysis accuracy of the characteristic data of the three-dimensional construction of grassland landforms was higher than that of the traditional two-dimensional plane construction [5]. Although the 3D reconstruction of grassland landforms can accurately analyze the grassland geological structure, it lacks intelligent technology to assist.

The intelligent robot vision system can realize accurate spatial positioning analysis, and apply the intelligent robot vision system to the three-dimensional construction of grassland landforms. Among them, Zhang Y achieved 3D reconstruction of grassland landforms through binocular vision technology, which improved the accuracy of 3D construction [6]. Cheng C's research showed that intelligent robot vision can denoise 3D reconstruction, improving the stability of 3D construction [7]. Park S proposed a robot that runs two cameras simultaneously for 3D construction, and an accurate 3D model can be obtained by analyzing the eigenvalues [8]. Wang J's research pointed out that the intelligent computer vision system can effectively construct three-dimensional grassland landforms by using rectangular feature detection [9]. Although intelligent robotic vision systems can improve the accuracy of 3D construction, there is a lack of comparison with traditional grassland landform surveys.

Surveying grassland landforms is an effective supervision measure for grassland ecological environment, which can analyze the complex geological structure of grassland landforms. Using the intelligent robot vision system, the grassland landform was reconstructed in 3D, and its characteristic values were simulated and analyzed. Compared with the traditional 3D modeling of grassland landforms, the grassland landforms based on the intelligent robot vision system can effectively improve the accuracy of data construction [10].

2 Related works

In recent years, technological advances have had a substantial impact on a variety of sectors, especially monitoring of the environment and landform assessment. Numerous studies have investigated various approaches for assessing soil parameters, detecting landforms, and reconstructing three-dimensional models of natural and artificial structures. This relevant work to emphasize advances and constraints of existing methodologies, emphasizing the requirement for creative approaches in the area of 3D reconstruction of grassland landforms.

Table 1: Overview of related research in environmental tracking and landform assessment

Reference No	Objective	Methodology	Result	Limitations
[11]	To assess the chemical characteristics of reclaimed soil in an arid grassland mining location.	Variance, correlation, and principal component analysis are used to evaluate soil characteristics and spatial-temporal variations.	Reclamation enhanced soil chemical characteristics, and surface soil health enhanced with time.	Constrained to a particular mining location; may not apply to other places.
[12]	To create a semi-automated object-based image analysis (OBIA) method for desert landform discovery and modeling.	Using DEM and spectral data, a multi-resolution segmentation method and object-based rule sets are applied.	Desert landforms were detected and classified with excellent accuracy (96.21%-95.05%).	Concentrated on desert landscapes, not directly relevant to grasslands.
[13]	Determine 3D macropore networks in forest soils and compare them to agriculture and grasslands soils.	X-ray computed tomography and image analytics for soil columns	Comprehensive measurement of macropore networks in soils from forests, with strong interconnectedness and vertical consistency	Particular to forest soils; not directly tackling grassland landscapes.
[14]	To recreate scaffolds from a	Data-driven approach involving	Over 70% accuracy in recreating scaffolding	Concentrated on construction areas,

	photogrammetric point cloud of building sites, utilizing a unique 3D local feature description.	preprocessing, classification, and geometric modeling with the LSSHOT descriptor.	elements; excellent noise management	may not directly applicable to natural landscape reconstruction.
[15]	Create an interpolation algorithm for dynamic 3D face rebuilding.	Automated iterative interpolation algorithm for point cloud data.	Excellent saturability and thoroughness in 3D facial feature rebuilding.	Particular to facial recognition and not immediately associated with geological surveys.
[16]	To present a 3D machine vision-enabled smart robot architecture	Automated calibration of monocular and binocular cameras, 3D placement utilizing binocular vision.	Efficient binocular 3D location in simple situations and a stable system	Restricted to controlled surroundings, may struggle with complicated natural landscape.
[17]	To create a scheme for natural grassland-type recognition utilizing deep learning.	PyTorch deep learning system with transfer learning from VGG-19 and data augmentation	Optimum grassland identification model with excellent accuracy	Depending on the quality of images and field data, it might not include all grassland types.
[18]	To create a smart grazing solution for unmanned animal husbandry.	Incorporation of remote sensing, Internet of Things, and machine learning	Effective grazing approach for better utilization of resources	Concentrated on animal husbandry, not directly tackling geological landscape rebuilding.
[19]	To develop a QR code-based interior navigation system for attendant robots.	QR code geolocation and planning of paths algorithms.	Efficient indoor navigation for robots, with great accuracy	Limited to interior surroundings; not suited for large-scale outside surveys.
[20]	To enhance object detection in robot vision, discriminative bit selection hashing	RGB-D object detection using the bit selection hashing approach	Enhanced object recognition accuracy in robotic vision systems.	Particular to object identification, does not deal with large-scale landform analytics.

The evaluated works show a wide range of methodology and uses in ecological tracking and landform assessment, including soil property assessment, sophisticated image evaluation, and 3D reconstruction methods. While each study provides useful insights, constraints such as a focus on particular areas, settings, or architecture highlight the need for more flexible and broad techniques. The suggested work uses a smart robot vision system to tackle these constraints, giving a better solution for precise and efficient 3D reconstruction of grassland landscapes.

2.1 Three-dimensional reconstruction method of grassland landform

Grassland landform is a kind of ecological environment. The reason for the formation of grassland landform is that the soil layer is thin and the precipitation is less, so that most herbs cannot grow. The structure of grassland landforms is complex and

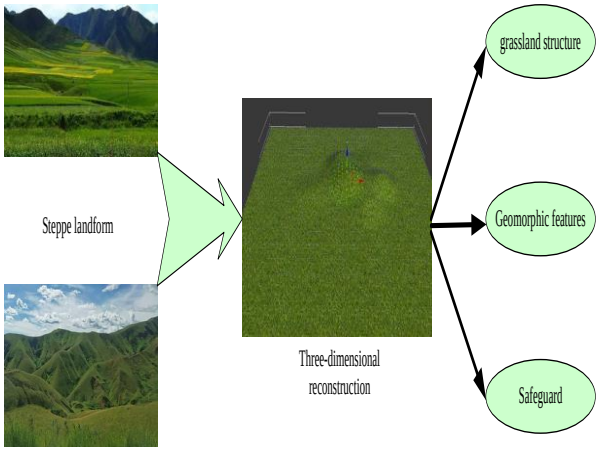

Figure 1: Process map of 3D reconstruction of grassland landforms

changeable. By 3D reconstruction of grassland landforms, the data characteristics of grassland landforms can be obtained, so as to protect grassland resources in a targeted manner. The 3D reconstruction process of the grassland landform is shown in Figure 1.

The three-dimensional image analysis approach necessitates a simulation to validate the suggested rationality of the three-dimensional vision-based distribution of grassland landform. A simulation platform for three-dimensional image analysis is developed under the Windows 10 environment to ensure that landscape gardens and grassland landform are distributed rationally. The Point Grey Flea2 camera was utilized, and the experimental data set consisted of fifty frames of photos supplied by the Association of Landscape Architecture. The resolution of the camera was 640pi × 520pi. The experimental PC host is equipped with the following hardware: a 3.0GHz Intel Core i5 8500 quad-core processor, 8 GB of RAM, a 4 GB Nvidia GTX970 graphics card, and a 500 GB hard drive. Adobe Photoshop CS6, Auto CAD for 3D drawings, and SketchUp for 3D models are some of the platforms utilized.

In Figure 1, the 3D reconstruction process of the grassland landform is as follows: photographing the grassland landform with a camera, extracting feature points, and using a feature matching algorithm to construct the grassland landform in 3D. Finally, according to the constructed three-dimensional model, the structure and characteristics of grassland landforms can be analyzed, and corresponding grassland protection measures can be formulated according to the landform characteristics.

Extraction of 3D Features: The first step in 3D reconstruction of grassland landforms is to extract 3D features of grassland landforms, which is based on camera vision by analysing information that is salient and less likely to be lost in the grassland images captured by the camera. The 3D features of grasslands are mainly divided into three types: point, line, and flat.

The matching of three-dimensional features is the premise of feature extraction. At present, the common three-dimensional feature matching is mainly through grayscale matching, and by establishing a window model. The feature matching search is performed at the center of the image. Before feature extraction, it is necessary to determine the position of the camera, and try to ensure that the brightness of each pixel of the grassland landform image is related to the intensity of the reflected light on its surface. There are two types of camera shooting: fixed camera shooting and motion camera shooting.

Stereoscopic vision of grassland landforms can be obtained through different grassland angles captured by multiple cameras, and three-dimensional information of grassland landforms can be obtained through the deviation of image pixel positions under the vision of different cameras. The principle of grassland stereo vision is shown in Figure 2.

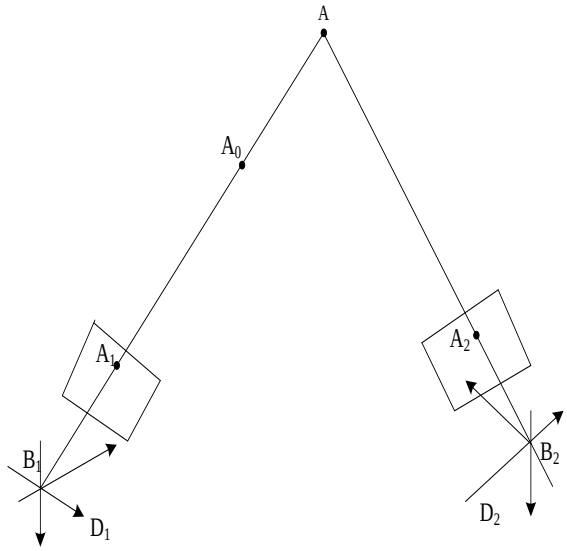

Figure 2: Schematic diagram of grassland stereo vision

In Figure 2, assuming that there are two grassland landform photographing cameras B_1 and B_2, and A is any point in the grassland landform space, A_1 and A_2 are the imaging points of point A in the two cameras respectively. Observing point, A from the perspectives of two different cameras, there can be two paths B_1A and B_2A, but there is a common point A under the perspectives of the two cameras, so point A is a 3D point under the camera perspective.

The principle of 3D stereo measurement is as follows. Assuming that the projection matrices of cameras B_1 and B_2 are R_1 and R_2 respectively, and the coordinates of point A in the coordinate systems of the two camera perspectives are $A_1(a_1, b_1)$ and $A_2(a_2, b_2)$ respectively, the following relationship can be obtained:

$$ZD_1\begin{bmatrix} a_1 \\ b_1 \\ 1 \end{bmatrix} = \begin{bmatrix} r_1^{11} & r_1^{12} & r_1^{13} & r_1^{14} \\ r_1^{21} & r_1^{22} & r_1^{23} & r_1^{24} \\ r_1^{31} & r_1^{32} & r_1^{33} & r_1^{34} \end{bmatrix}\begin{bmatrix} X \\ Y \\ Z \\ 1 \end{bmatrix} \quad (1)$$

In Formula (1), D_1 is the abscissa in the camera B_1. Similarly, the coordinate relationship under camera B_2 can be obtained.

$$ZD_2\begin{bmatrix} a_2 \\ b_2 \\ 1 \end{bmatrix} = \begin{bmatrix} r_2^{11} & r_2^{12} & r_2^{13} & r_2^{14} \\ r_2^{21} & r_2^{22} & r_2^{23} & r_2^{24} \\ r_2^{31} & r_2^{32} & r_2^{33} & r_2^{34} \end{bmatrix}\begin{bmatrix} X \\ Y \\ Z \\ 1 \end{bmatrix} \quad (2)$$

Combining Formula (1) and Formula (2), Formula (3) can be obtained:

$$(a_1 r_1^{31} - r_1^{11})X + (a_1 r_1^{32} - r_1^{12})Y + (a_1 r_1^{33} - r_1^{13})Z = r_1^{14} - a_1 r_1^{34} \quad (3)$$

Through Formula (3), the values of X, Y, and Z can be obtained, so that the three-dimensional coordinates of any point in the grassland landform can be obtained.

Point feature extraction algorithm

The image features of grassland landforms are data that can effectively reflect the features of grassland landforms. By analyzing the characteristic data, the calculation amount of 3D reconstruction can be reduced, and a lot of non-feature memory can be saved. The traditional 3D feature extraction method is point feature extraction.

By calculating the gradient of each pixel in the grassland landform image, and calculating the point with the maximum value of the two gradient directions, the detection process of point feature extraction is as follows:

$$Q = \det(P) - k[ur(P)]^2 \quad (4)$$

In Formula (4), when the value of Q exceeds the set interval, Q is the feature point. P represents a pixel in the grassland landscape.

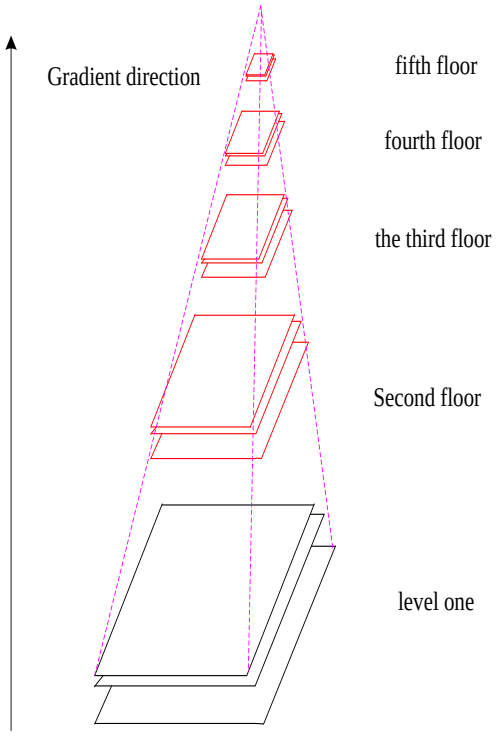

Figure 3: Process diagram of point feature extraction

The process of point feature extraction is shown in Figure 3.

In Figure 3, by continuously extracting pixel gradient feature points, feature points that can summarize the measured image can be extracted after multiple feature extractions, and finally the grassland landform can be reconstructed with the feature points.

2.2 Intelligent robot vision technology

The intelligent robot vision system combines visual analysis, three-dimensional construction with robots, with the functions of autonomous positioning and intelligent analysis, which can be effectively applied to 3D reconstruction of grassland landforms.

In the three-dimensional reconstruction of the intelligent robot vision system, the image problem in motion needs to be considered. During the movement of the robot, the camera worn by the robot can rotate and shake to different degrees. It is necessary to effectively analyze the feature data during 3D reconstruction. The structure of the feature extraction

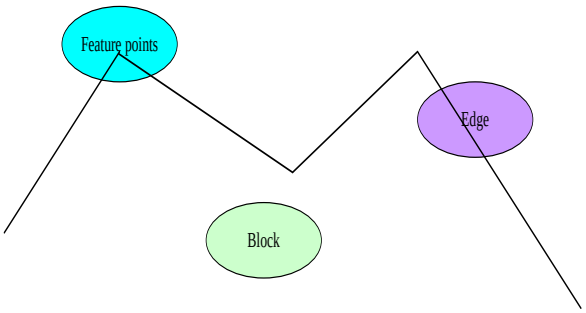

Figure 4: Structure diagram of feature extraction

of the intelligent robot vision system is shown in Figure 4.

In Figure 4, the structure of feature extraction is mainly divided into feature points, blocks and edges. Uncertainty analysis of image rotation is mainly implemented in the form of determining feature points. The selection of feature points is mainly through the analysis of the centroid point of the image.

The moment of A in a grassland image A is supposed to be expressed as Formula (5):

$$r_{a,b} = \sum_{x,y \in A} x^a y^b \tag{5}$$

In Formula (5), the value range of a and b is $\{0,1\}$.

Using the moments of image A, the centroid of image A can be found:

$$S = (\frac{r_{10}}{r_{00}}, \frac{r_{01}}{r_{00}}) \tag{6}$$

In Formula (6), S represents the centroid of the image A. Supposing that the geometric center of image A be point G, then the feature vector is GS, and the direction of the feature point can be obtained.

$$\theta = acr\tan(\frac{r_{01}}{r_{10}}) \tag{7}$$

In the process of feature point extraction, the intelligent robot vision system can determine the angle of the feature point, thereby determining the position of the feature point, and improving the stability and accuracy of processing grassland landform images.

3 Three dimensional reconstruction experiment and result

3.1 Three-dimensional reconstruction experiment of grassland landform

3D Reconstruction Data of Grassland Landforms: Three-dimensional reconstruction of grassland landforms is a data analysis of grassland landforms, which is conducive to accurately studying the structural composition of grasslands and the stability of grassland ecosystems. To carry out 3D reconstruction analysis of grassland landforms, it is necessary to establish an index that can be used to evaluate the effect of 3D reconstruction of grassland landforms. For this purpose, the experiment conducted statistics on the close contacts in the 3D reconstruction system of grassland landforms [21]. Table 2 shows the personnel involved in the analysis of grassland landforms.

Table 2: Information about the personnel involved in the analysis of grassland landforms

Serial number	Person type	Number of people (person)	Proportion
1	Prairie landscape surveyor	80	32%
2	3D reconstruction technician	90	36%
3	Grassland landform photographer	80	32%

In Table 2, the survey data of relevant personnel in the 3D reconstruction of grassland landforms are described. The survey objects were divided into three categories, namely grassland landform surveyors, 3D reconstruction technicians, and grassland landform photographers. The largest number of people were 3D reconstruction technicians, with the proportion of 36%.

A questionnaire survey was conducted on the above-mentioned close contacts of the grassland landforms, and the evaluation indicators of the three-dimensional reconstruction of the grassland landforms were mainly counted, as well as the proportion of the number of people each index accounted for [22]. The statistical results of the evaluation indicators for the above 250 people are shown in Table 3.

Table 3: Statistical results of evaluation indicators

Serial	Evaluation	Number	Proportion

number	indicators	of people (person)	
1	Accuracy of 3D Reconstruction	65	26%
2	Feature data matching degree	60	24%
3	Noise Immunity for 3D Reconstruction	55	22%
4	3D reconstruction time	60	24%
5	Memory required for 3D reconstruction	10	4%

In Table 2, a total of 5 evaluation indicators were counted, of which the accuracy indicator of 3D reconstruction had the largest proportion, with the proportion of 26%. The smallest proportion was the memory index required for 3D reconstruction, which accounted for 4%. Due to the large amount of memory that can be endured when reconstructing grassland landforms, the memory space required for 3D reconstruction had little effect on 3D reconstruction. Therefore, the first four indicators in Table 2 were used as indicators for evaluating the effect of 3D reconstruction of grassland landforms [23].

Design Process of 3D Reconstruction of Grassland Landforms: In order to analyze the effect of 3D reconstruction of grassland landforms based on the intelligent robot vision system, a comparison and analysis was made with the traditional 3D reconstruction of grassland landforms. Among them, the traditional 3D reconstruction adopted point feature extraction algorithm for analysis. In order to ensure the accuracy of the two 3D reconstruction comparison experiments, the experimental environment of the two 3D reconstruction methods must be the same, and the same grassland landform must be analyzed.

In order to ensure the vastness and diversity of grassland landforms, the experiment took the Qinghai-Tibet grassland area in China as an example. When comparing the two 3D reconstruction methods, in order to ensure the integrity of the comparison experiment, the experiment set up grassland areas of different sizes for analysis. Experiments were performed on a square area with a side of 2km and a square area with a side of 4km [24].

In the process of 3D reconstruction of grassland landforms, the data of one experiment was serendipitous. To this end, the experiment carried out the three-dimensional reconstruction process for several times for the comparison test of the two three-dimensional reconstructions, which was set to 1st, 2nd, 3rd, 4th, 5th and 6th, and observed the effects of the two three-dimensional reconstructions under each number of times.

3.2 Results of 3D reconstruction comparison experiments

Accuracy of 3D Reconstruction: The effect of 3D reconstruction is mainly determined by the accuracy of 3D reconstruction. The higher the accuracy of 3D reconstruction, the better the effect of 3D reconstruction of grassland landforms. The basis for judging the accuracy of 3D reconstruction is the similarity between the grassland landform after 3D modeling and the actual grassland landform. The 3D reconstruction accuracy of the 3D reconstruction of the two grassland landforms was compared, in which six comparison results were set. The comparison results of the accuracy of the 3D reconstruction of the two grassland landforms are shown in Figure 5.

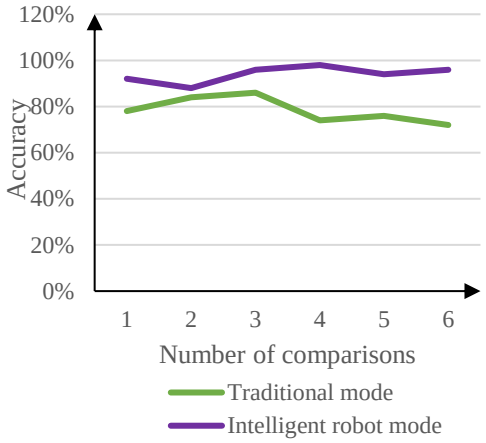

(a) Square grassland with a side of 2km

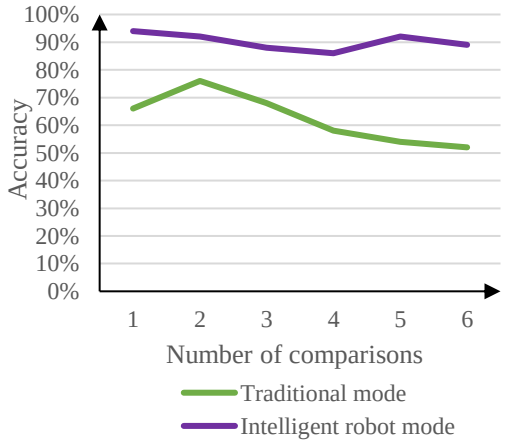

(b) Square grassland with a side of 4km

Figure 5: 3D reconstruction accuracy comparison results

In Figure 5(a), a comparison of two 3D reconstruction methods is depicted on a square grassland with a side of 2 km. In the traditional 3D reconstruction method, the accuracy of 3D reconstruction first increased and then decreased during the six experiments, while the accuracy of grassland 3D reconstruction based on intelligent robot vision system generally showed an upward trend. In the sixth experiment, the accuracies of the two 3D reconstructions were 72% and 96% respectively. In Figure 5(b), the 3D reconstruction accuracy experiment was performed on a square grassland area with a side of 4km. The accuracy of the traditional 3D reconstruction of grassland landforms changed significantly, which started to drop after the second experiment, while the accuracy of the 3D reconstruction based on the intelligent robot vision system did not change much. In the sixth experiment, the accuracies of the two 3D reconstructions were 52% and 89% respectively. Therefore, the 3D reconstruction of grassland based on intelligent robot vision system can effectively improve the accuracy of 3D reconstruction.

Matching Degree of Feature Data: The three-dimensional reconstruction of grassland landforms is mainly through matching and analysis of feature data, and the feature data matching of traditional three-dimensional reconstruction methods adopts point feature extraction and matching technology. The 3D reconstruction of the intelligent robot vision system uses intelligent robot vision technology for feature matching. The matching degree of feature data was compared between the two 3D reconstruction methods, and was compared for 6 times in the experiment. The comparison result of the matching degree of feature data is shown in Figure 6.

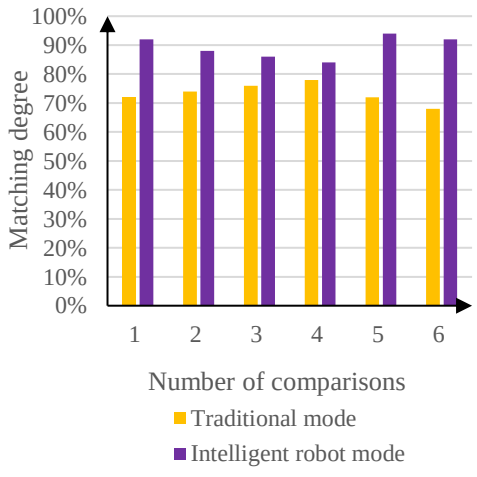

(a) Square grassland with 2km side

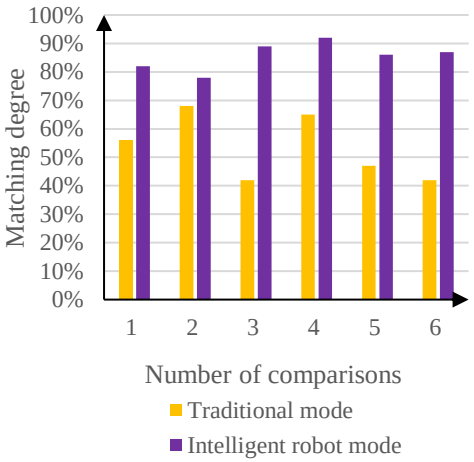

(b) Square grassland with 4km side

Figure 6: Comparison result of feature data matching degree

In Figure 6(a), it was a comparison of characteristic data of three-dimensional reconstruction in a square grassland area with a side of 2 km. The experiments were carried out 6 times, and the matching degree of the characteristic data of the traditional 3D reconstruction of grassland landforms was lower than that of the intelligent robot vision system. In the six comparison results, the average matching degrees of the two 3D reconstruction feature data were 73.3% and 89.3% respectively. In Figure 6(b), the grassland landform compared in the experiment was a square grassland with a side of 4km. The difference in the characteristic data of the two 3D reconstruction methods was more obvious. The average matching degree of the characteristic data of the two 3D reconstruction methods was 53.3% and 85.7% respectively. Therefore, applying the intelligent robot vision system to the 3D reconstruction of grassland landforms can improve the matching degree of feature data [25].

Noise Immunity for 3D Reconstruction: During 3D reconstruction of grassland landforms, it can be affected by many factors, including camera shooting errors, feature data positioning errors, etc., which affect the effect of 3D reconstruction. The noise resistance of 3D reconstruction is the embodiment of the stability of 3D reconstruction. The two 3D reconstruction methods were used for 6 experiments on two different grassland areas, and the noise immunity of two types of 3D reconstructions was compared. The comparison results of noise immunity of 3D reconstruction are shown in Figure 7.

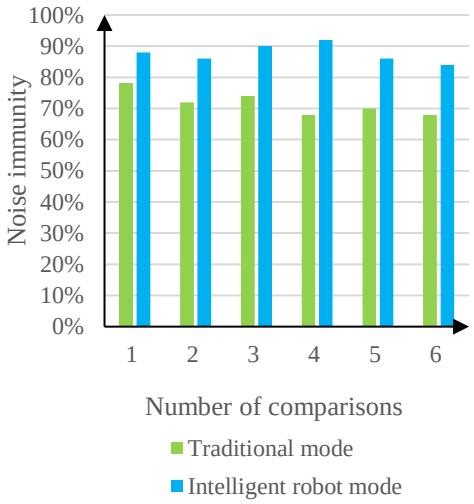

Figure 7: Comparison results of 3D reconstruction noise immunity

In Figure 7, the overall data fluctuation of the three-dimensional reconstruction of the two grassland landforms was not large under the results of the six experiments. However, the six experimental data results were based on the intelligent robot vision system, and the noise immunity of 3D reconstruction was greater than that of traditional 3D reconstruction. Among them, in the fourth experiment, the difference in noise immunity between the two was the largest, and the traditional three-dimensional noise immunity at this time was 68%, while the noise immunity of 3D reconstruction based on intelligent robot vision system was 92%. In the first set of experiments, the noise immunity of the two 3D reconstruction methods was the smallest, with a difference of 10%. Therefore, the intelligent robot vision system can improve the noise resistance of 3D reconstruction of grassland landforms.

Time of 3D Reconstruction: The time required for 3D reconstruction refers to the time required to complete the entire process from camera shooting and framing to feature data matching to 3D modeling [26-27]. The time of 3D reconstruction of grassland landform reflects the efficiency of 3D reconstruction. The shorter the time of 3D reconstruction, the higher the

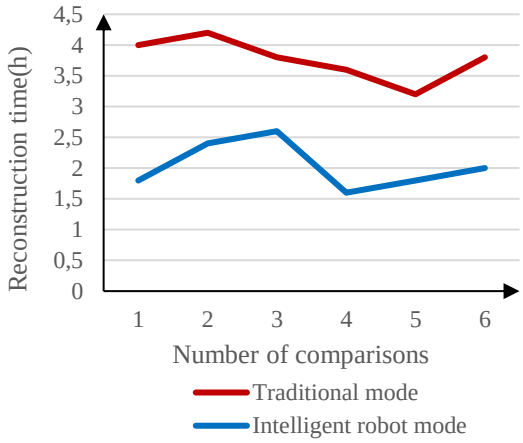

(a) Square grassland with 2km side

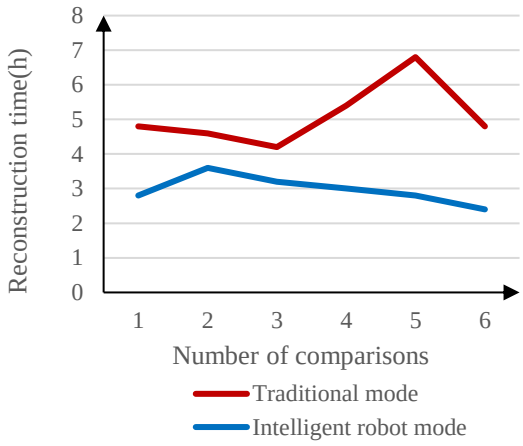

(b) Square grassland with 4km side

Figure 8: Comparison of 3D reconstruction accuracy results

efficiency of 3D modeling. The time required for two 3D reconstructions of grassland landforms was compared, and the comparison results of 3D modeling reconstruction time are shown in Figure 8.

In Figure 8(a), it shows the time required for two 3D reconstruction methods to perform 3D reconstruction on a square grassland with a side of 2km. Among them, the traditional 3D reconstruction time was 3.2 hours at the lowest, 4.0 hours at the highest, and 3.8 hours on average during the six tests, while the minimum time required for 3D reconstruction based on the intelligent robot vision system was 1.6 hours and the maximum was 2.6 hours, with the average of 2.0 hours. In Figure 8(b), a square grassland with a side of 4km was used as the experimental area, and the time required for the 3D reconstruction based on the intelligent robot vision system was significantly shorter than that of the traditional 3D reconstruction. In the fifth test, the time

required for the two 3D reconstructions differed the most, with a difference of 4.0 hours. Therefore, the 3D reconstruction of grassland landforms based on the intelligent robot vision system can greatly shorten the time of 3D reconstruction and improve the efficiency of 3D reconstruction of grassland landforms.

Taking everything into account, the system has shown to be quite stable, which is crucial for ensuring accurate and precise image recognition. However, it is clear that the loading speed is affecting the system's access speed. Given the wide range of image recognition functions, there is no one-size-fits-all solution when it comes to meeting the function's individual criteria. Ultimately, it is necessary to integrate and present the data from all functions together, and progress will be hindered by specific slower processing functions. Alternatively, when it comes to server indicators, specific cluster indices could vary depending on server characteristics and regional network conditions. These discrepancies are now within a more manageable range, but there is room for improvement. As a whole, there is room for improvement in all of this system's modules.

4 Conclusion

The three-dimensional reconstruction of grassland has a positive effect on exploring the landform structure of grassland and promoting the development of grassland. In this paper, the intelligent robot vision system was applied to the 3D reconstruction of grassland landforms, and the efficiency of 3D reconstruction was improved by optimizing the matching of grassland landform feature data. By comparing with the traditional 3D reconstruction of grassland landforms, the experimental results showed that the application of the intelligent robot vision system to the 3D reconstruction of grassland landforms can effectively improve the accuracy of 3D reconstruction, and improve the matching degree of feature data and the stability of 3D reconstruction. The efficiency of 3D reconstruction can be improved by the matching and optimization of characteristic data through intelligent technology, which can not only conduct more detailed analysis of the grassland landform structure, but also predict the development trend of the grassland ecological environment, as well as protect and develop the grassland ecological environment in a targeted manner. However, the comparison of the two 3D reconstructions in this paper was only limited to the square grassland area with side lengths of 2 km and 4 km, and no comparison was made for larger or smaller grassland areas. Therefore, expanding the grassland area for the comparison of the two 3D modeling methods is the direction of future research.

Data availability

The data used to support the findings of this study are available from the corresponding author upon request.

Conflicts of interest

The authors declare no conflicts of interest.

Funding statement

This research study is sponsored by Hebei Provincial Department of Education Youth Top Talent Project. The name of the project is Characteristics of near-surface wind field of grassland landform and wind resistance performance of photovoltaic panels. The project number is BJ202010. Thank the project for supporting this article!

References

[1] Ko J H, 2020 “Robot Vision System based on 3D Depth map and Object Recognition”, *Journal of the Institute of Electronics and Information Engineers*, vol.57, no.3, pp.101-105..

[2] Park D , Kang K M , Bae J W , Han J H, 2019. “Robot Vision to Audio Description Based on Deep Learning for Effective Human-Robot Interaction”, *The Journal of Korea Robotics Society*, vol.14, no.1, pp.22-30.

[3] Kim J M , Choi C W , Jang W S, 2018. “Development of Robot Vision Control Schemes based on Batch Method for Tracking of Moving Rigid Body Target”, *Journal of the Korean Society of Manufacturing Process Engineers*, vol.17, no.5, pp.161-172.

[4] Cao T Y , Cai H Y , Fang D M , Liu C, 2017. “Robot vision system for keyframe global map establishment and robot localization based on graphic content matching”, *Guangxue Jingmi Gongcheng/Optics and Precision Engineering*, vol.25, no.8, pp.2221-2232.

[5] Wang J , Tang J , Guo T , Zhang S , Xia W , Tan H , et al, 2019. “C3N4-digested 3D construction of hierarchical metallic phase MoS2 nanostructures”, *Journal of Materials Chemistry A*, vol.7, no.31, pp.18388-18396.

[6] Chen C , Tang L , Hancock C M , Zhang P, 2019. “Development of low-cost mobile laser scanning for 3D construction indoor mapping by using inertial measurement unit, ultra-wide band and 2D laser scanner”, *Engineering Construction & Architectural Management*, vol.26, no.7, pp.1367-1386.

[7] Roslan A F , Salehuddin F , Zain A , Kaharudin K E , Maheran A, 2018. “30nm DG-FinFET 3D construction impact towards short channel effects”, *Indonesian Journal of Electrical Engineering and Computer Science*, vol.12, no.3, pp.1358-1365.

[8] Asa K , Funabora Y , Doki S , Doki K, 2017. “Automatic Measuring Position Determination of

UAVs for Visual Inspection System of Infrastructures Based on 3D Construction Model Considering Accuracy of Data", *Transactions of the Society of Instrument & Control Engineers*, vol.53, no.3, pp.229-235.

[9] Mukundan R, 2017. "Contour Based High Resolution 3D Mesh Construction Using HRCT and MRI Stacks", *International journal of multimedia data engineering & management*, vol.8, no.4, pp.60-73.

[10] Patil M C , Patil S S, 2020. "3D Construction of Brain using 2D MRI Slices", *Gender Technology and Development*, vol.9, no.4, pp.2278-3075.

[11] Huang Y , Kuang X , Cao Y , Bai Z, 2018. "The soil chemical properties of reclaimed land in an arid grassland dump in an opencast mining area in China", *RSC Advances*, vol.8, no.72, pp.41499-41508.

[12] Sun R , Xu W D , Chen W , Zhang Y, 2017. "The quantitative characteristics of plant germplasm resources in Horqin grassland", *Chinese Journal of Ecology*, vol.36, no.10, pp.2699-2706.

[13] Zhang J M , Xu Z M , Li F , Hou R J , Ren Z, 2017. "Quantification of 3D macropore networks in forest soils in Touzhai valley(Yunnan, China) using X-ray computed tomography and image analysis", *Journal of Mountain Science*, vol.14, no.3, pp.474-491.

[14] Xu Y , Tuttas S , Hoegner L , Stilla U, 2018. "Reconstruction of scaffolds from a photogrammetric point cloud of construction sites using a novel 3D local feature descriptor", *Automation in construction*, vol.85, no.1, pp.76-95.

[15] Sui D , Hou D , Duan X, 2017. "An interpolation algorithm fitted for dynamic 3D face reconstruction", *Multimedia Tools and Applications*, vol.76, no.19, pp.19575-19589.

[16] Zhang Y , Zhao J , Han H, 2021. "A 3D Machine Vision-Enabled Intelligent Robot Architecture", *Mobile Information Systems*, vol.2021, no.3, pp.1-11.

[17] Cheng C , Guo X , Chen X , Li C , Xiong H, "Control System Development of Intelligent Robot Based on Mindstorms", *Wuhan Ligong Daxue Xuebao (Jiaotong Kexue Yu Gongcheng Ban)/Journal of Wuhan University of Technology (Transportation Science and Engineering)*, vol.42, no.2, pp.247-252, 2018.

[18] Park S, 2018. "Computational Vision for Automatic Tracking and Objective Estimation of Mobile Robot Trajectory", *Journal of Computer Sciences and Applications*, vol.6, no.1, pp.17-22.

[19] Wang J , Xiao X, 2018. "Mobile robot integrated navigation method based on QR code vision positioning", *Chinese Journal of Scientific Instrument*, vol.39, no.8, pp.230-238.

[20] Feng L , Liu Y , Li Z , Zhang M , Wang F , Liu S , et al, 2019. "Discriminative bit selection hashing in RGB-D based object recognition for robot vision", *Assembly Automation*, vol.39, no.1, pp.17-25.

[21] Borges F , Fernandes R , Silva I N , Silva C B S, 2017. "Feature Extraction and Power Quality Disturbances Classification Using Smart Meters", *IEEE Transactions on Industrial Informatics*, vol.12, no.2, pp.824-833.

[22] You M , Wang H , Liu Z , Chen C , Liu J , Xu X H , et al, 2017. "Novel feature extraction method for cough detection using NMF", *Iet Signal Processing*, vol.11, no.5, pp.515-520.

[23] Mo D , Lai Z , Wong W, 2019. "Locally Joint Sparse Marginal Embedding for Feature Extraction", *IEEE Transactions on Multimedia*, vol.21, no.12, pp.3038-3052.

[24] Hang R , Liu Q , Sun Y , Yuan X , Pei H , Plaza A , et al, 2017. "Robust Matrix Discriminative Analysis for Feature Extraction From Hyperspectral Images", *IEEE Journal of Selected Topics in Applied Earth Observations and Remote Sensing*, vol.10, no.5, pp.2002-2011.

[25] Jung J Y , Kim S W , Yoo C H , Park W J , Ko S J, 2017. "LBP-ferns-based feature extraction for robust facial recognition", *IEEE Transactions on Consumer Electronics*, vol.62, no.4, pp.446-453.

[26] Jurczyk-Bunkowska M, 2021. "Tactical manufacturing capacity planning based on discrete event simulation and throughput accounting: A case study of medium sized production enterprise", *Advances in Production Engineering & Management*, vol. 16, no. 3, pp.335-347.

[27] Zhang Y D , Liao L , Yu Q , Ma W G , Li K H, 2021. "Using the gradient boosting decision tree (GBDT) algorithm for a train delay prediction model considering the delay propagation feature", *Advances in Production Engineering & Management*, vol. 16, no. 3, pp.285-296.